Hypoxia triggers a proangiogenic pathway involving cancer cell microvesicles and PAR-2–mediated heparin-binding EGF signaling in endothelial cells

Katrin J. Svensson[a], Paulina Kucharzewska[a], Helena C. Christianson[a], Stefan Sköld[b], Tobias Löfstedt[c], Maria C. Johansson[a], Matthias Mörgelin[d], Johan Bengzon[e], Wolfram Ruf[f], and Mattias Belting[a,b,1]

[a]Department of Clinical Sciences, Section of Oncology, Lund University, SE-221 85 Lund, Sweden; [b]Department of Oncology, Skåne University Hospital, SE-221 85 Lund, Sweden; [c]BioInvent International, SE-223 70 Lund, Sweden; [d]Department of Clinical Sciences, Section of Clinical and Experimental Infectious Medicine, Lund University, SE-221 84 Lund, Sweden; [e]Department of Clinical Sciences, Section of Neurosurgery, Skåne University Hospital, S-221 85 Lund, Sweden; and [f]Department of Immunology and Microbial Science, The Scripps Research Institute, La Jolla, CA 92037

Highly malignant tumors, such as glioblastomas, are characterized by hypoxia, endothelial cell (EC) hyperplasia, and hypercoagulation. However, how these phenomena of the tumor microenvironment may be linked at the molecular level during tumor development remains ill-defined. Here, we provide evidence that hypoxia up-regulates protease-activated receptor 2 (PAR-2), i.e., a G-protein–coupled receptor of coagulation-dependent signaling, in ECs. Hypoxic induction of PAR-2 was found to elicit an angiogenic EC phenotype and to specifically up-regulate heparin-binding EGF-like growth factor (HB-EGF). Inhibition of HB-EGF by antibody neutralization or heparin treatment efficiently counteracted PAR-2–mediated activation of hypoxic ECs. We show that PAR-2–dependent HB-EGF induction was associated with increased phosphorylation of ERK1/2, and inhibition of ERK1/2 phosphorylation attenuated PAR-2–dependent HB-EGF induction as well as EC activation. Tissue factor (TF), i.e., the major initiator of coagulation-dependent PAR signaling, was substantially induced by hypoxia in several types of cancer cells, including glioblastoma; however, TF was undetectable in ECs even at prolonged hypoxia, which precludes cell-autonomous PAR-2 activation through TF. Interestingly, hypoxic cancer cells were shown to release substantial amounts of TF that was mainly associated with secreted microvesicles with exosome-like characteristics. Vesicles derived from glioblastoma cells were found to trigger TF/VIIa–dependent activation of hypoxic ECs in a paracrine manner. We provide evidence of a hypoxia-induced signaling axis that links coagulation activation in cancer cells to PAR-2–mediated activation of ECs. The identified pathway may constitute an interesting target for the development of additional strategies to treat aggressive brain tumors.

angiogenesis | exosome | glioma

G lioblastoma multiforme (GBM) is the most deadly of primary brain tumors, with a median survival of only 15 mo after diagnosis even with the most recent combination treatments, which includes surgery, radiochemotherapy, and adjuvant chemotherapy (1). The aggressiveness of GBM has been correlated with severe hypoxia (2), resulting in large areas of necrosis and an extensive, hyperpermeable vasculature, i.e., the histopathological characteristics of these tumors (1). Hypoxic activation is a hallmark of growing tumors as a result of inadequate oxygen supply, and increased angiogenesis serves to restore the supply of nutrients and oxygen to the tumor environment (3). GBM is further characterized by the activation of the coagulation system, and intravascular thrombosis exacerbates intratumoral hypoxia, abnormal endothelial cell (EC) proliferation, and tumor necrosis (4).

The hypercoagulative activity of malignant tumors has been associated with the overexpression of tissue factor (TF), a 47-kDa cell membrane intercalated protein that plays a key role in the initiation of the coagulation cascade (5, 6). Experimental models of tumor development, as well as human cancer materials, link TF to the aggressiveness of several malignancies, including gliomas (5–7). TF induction in cancer cells may be driven by oncogenetic events, e.g., through EGF receptor (EGFR) and its mutant, EGFRvIII, and inactivation of the tumor suppressor PTEN (6, 8–10). Other reports have suggested that TF may be triggered by hypoxia through the transcription factor Early growth response gene-1 (11).

Importantly, TF has been shown to promote tumor development via cleavage activation of a unique class of G protein-coupled protease-activated receptors (PARs) (5, 6, 12). PARs are ubiquitously expressed in vascular and extravascular tissues, and TF-regulated PAR-2 signaling has been specifically linked to pathological angiogenesis of the retina (13, 14). Although these and other studies have suggested a specific involvement of PARs in angiogenesis, the exact function of TF-initiated coagulation signaling in the context of hypoxia-driven tumor angiogenesis remains ill-defined.

Here, we have investigated how the phenotypic characteristics of GBM, i.e., hypercoagulation, hypoxia, and abnormal angiogenesis, may be linked at the molecular level, and how hypoxia may coordinate the hypercoagulative activity of GBM cells and PAR-mediated angiogenic signaling.

Results

Hypoxic Induction of PAR-2 Signaling in ECs. We found a significant induction of PAR-2 mRNA in hypoxic compared with normoxic human umbilical vein ECs (HUVECs); however, expression of PAR-1—the other major receptor of coagulation proteases—was unaffected by hypoxia (Fig. 1A). Consistent with these results, PAR-2 protein was increased and remained up-regulated compared with normoxic control cells over the whole course (48 h) of the experiment (Fig. 1B). Similar results were obtained in HUAECs (to approximately 10-fold PAR-2 induction in hypoxic vs. normoxic cells; Fig. S1A) and in human brain microvascular ECs (HBMECs; to approximately 2.5-fold PAR-2 induction in hypoxic vs. normoxic cells; Fig. S1B). These results were corroborated by immunofluorescence staining for PARs in HUVECs
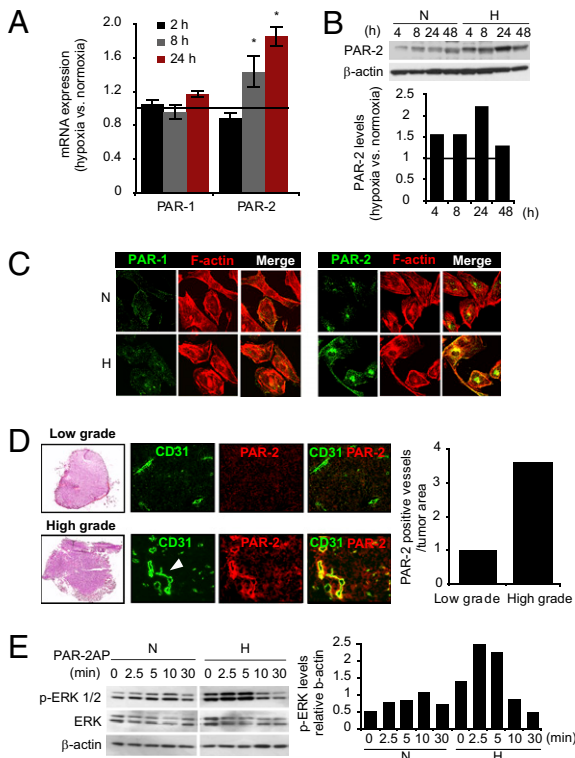
CELL BIOLOGY

Fig. 1. Hypoxia induces PAR-2 in ECs. (*A*) HUVECs were cultured at normoxia or hypoxia (1% O_2) for the indicated time periods, and PAR-1 and PAR-2 mRNA expression were determined by qRT-PCR as described in *SI Materials and Methods*. Results are presented as fold expression at hypoxia versus normoxia averaged from three separate experiments ± SD. (*Significant up-regulation vs. normoxia, P < 0.05.) (*B*) Hypoxia induces PAR-2 protein in ECs. HUVECs were cultured at normoxia (N) or hypoxia (H) for the indicated time periods, and PAR-2 and β-actin protein levels were determined in cell lysates by immunoblotting. *Lower*: Relative hypoxic PAR-2 levels [hypoxic (PAR-2/β-actin)/normoxic (PAR-2/β-actin)]; data shown are representative of at least three independent experiments. (*C* and *D*) Confocal fluorescence microscopy shows induction of PAR-2 in hypoxic ECs in vitro and in pathological vasculature of tumors from patients with GBM patient. (*C*) HUVECs were cultured at normoxia or hypoxia for 24 h, and then stained for PAR-1 or PAR-2 (green) and F-actin (phalloidin; red). (*D*) Serial cross-sections of fresh frozen patient tumor tissue from low-grade and high-grade astrocytoma were stained with H&E (*Left*) or analyzed by immunofluorescence microscopy by using rabbit anti–PAR-2 (red) and mouse anti-CD31 (EC/blood vessel marker; green) antibodies. PAR-2 coassociates with CD31 in typical dilated high-grade astrocytoma tumor vessels (white arrowhead). Images are representative of three separate tumors each of low grade (grade I and II) and high grade (grade IV) astrocytoma/GBM, obtained at 20× magnification. Quantification of PAR-2–positive vessels was performed on three cross-sections per tumor and adjusted for differences in tumor area by using ImageJ software. (*E*) PAR-2–dependent ERK1/2 phosphorylation (p-ERK) is enhanced in hypoxic ECs. Normoxic or hypoxic HUVECs were cultured for 24 h, followed by 16 h starvation in serum-free medium, and were then untreated (time point 0) or treated with the specific PAR-2AP SLIGKV (100 μM) for the indicated time periods, followed by immunoblotting for p-ERK, total ERK, and β-actin. *Right*: P-ERK/β-actin ratios from a representative experiment.

and HBMECs (Fig. 1*C* and Fig. S1*C*). Further, PAR-2 overexpression was demonstrated in pathological vasculature of patient high-grade astrocytoma/GBM tumors (Fig. 1*D* and Fig. S1*D*), whereas only few PAR-2–overexpressing vessels were found in low-grade astrocytoma (Fig. 1*D*). We found that hypoxia up-regulates cell-surface–located PAR-2 (Fig. S1*E*), and stimulation with the specific PAR-2 agonist peptide (PAR-2AP) SLIGKV (15, 16) resulted in significantly greater induction of

ERK1/2 phosphorylation [phosphorylated (p)–ERK1/2], a well known downstream readout of PAR-2 activation (5), in hypoxic compared with normoxic cells (Fig. 1*E*). These data provide evidence that hypoxia triggers signaling competent PAR-2 in ECs.

Hypoxia-Driven Angiogenesis Through PAR-2 Involves ERK1/2-Dependent Induction of HB-EGF. We next addressed the functional role of hypoxic induction of PAR-2 in angiogenesis. By using the scratch wound assay, we found that hypoxia per se appears to inhibit wound closure; treatment with a PAR-1–specific agonist peptide (TFLLRNPNDK) had no significant effect in normoxic or hypoxic conditions (Fig. 2*A*). Interestingly, PAR-2 activation was shown to substantially increase the number of hypoxic ECs in the wound area, whereas normoxic cells were unresponsive (Fig. 2*A*). These results may be explained by increased proliferation and/or migration of PAR-2–stimulated, hypoxic ECs. Indeed, activation of PAR-2, but not PAR-1, was shown to induce EC proliferation specifically at hypoxic conditions (Fig. 2*B*). Moreover, PAR-2 activation induced transwell migration of hypoxic ECs (Fig. 2*C*). At normoxia, ECs treated with siRNA against PAR-2 mRNA formed tube structures that were only partially disintegrated compared with cells treated with scrambled siRNA; however, PAR-2 knockdown in hypoxic cells resulted in a complete loss of EC tube structures (Fig. S2). Consistent with these results, RNAi-mediated PAR-2 deficiency was shown to increase the sensitivity of ECs to hypoxia-de-
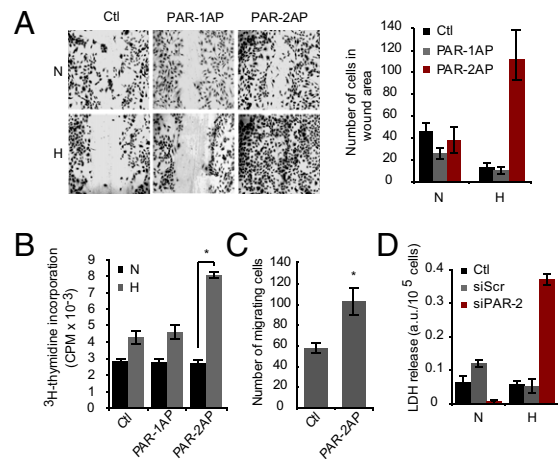

Fig. 2. Functional role of PAR-2 in hypoxia-driven angiogenesis. PAR-2 accelerates wound closure of hypoxic ECs. (*A*) Normoxic (N) or hypoxic (H) HUVECs were cultured for 24 h and starved for 16 h, and then a scratch wound was formed in confluent monolayers. The wound areas were captured after another 36 h of incubation with no treatment (Ctl) or treatment with PAR-1 agonist peptide TFLLRNPNDK (PAR-1AP; 100 μM) or PAR-2 agonist peptide (100 μM). Shown are representative images. *Right*: Quantitative analysis presented as the mean number of cells per wound area ± SD. (*B*) PAR-2 stimulates the proliferation of hypoxic ECs. HUVECs were cultured as in *A*, and were then untreated (Ctl) or treated with PAR-1AP (100 μM) or PAR-2AP (100 μM) for another 24 h in normoxia or hypoxia in the presence of 3 μCi/mL [³H]thymidine. Cell proliferation was determined by measurement of incorporated [³H]thymidine. (*Significant increase vs. control, P < 0.05.) (*C*) PAR-2 stimulates migration of hypoxic ECs. HUVECs were cultured in hypoxia and starved as in *A*, and were then seeded on transwell cell culture inserts in medium without (Ctl) or with PAR-2AP (100 μM). Results shown are the mean number of cells per field ± SD at 5 h of migration. (*D*) PAR-2 deficiency hypersensitizes ECs to hypoxia-induced cell death. Subconfluent HUVECs were transfected with siRNA specific for PAR-2 (siPAR-2) or with scrambled siRNA (siScr), followed by 24 h incubation under normoxic or hypoxic conditions. Knockdown of PAR-2 mRNA by siPAR-2 is shown in Fig. S2*A*. Cell media were then harvested and analyzed for LDH activity. Data presented as mean ± SD.

pendent cell death (Fig. 2D). These data indicate that induction of PAR-2 signaling has a functional role in hypoxia-driven angiogenesis.

As shown in Fig. 1E, p-ERK1/2 was significantly induced by PAR-2 activation in hypoxic ECs. Inhibition of p-ERK1/2 with UO126 counteracted PAR-2–dependent stimulation of hypoxic EC proliferation (Fig. S3). We next set out to determine whether PAR-2 may activate ECs through the induction of specific proangiogenic growth factors. As expected, hypoxia per se induced several angiogenesis-regulating molecules in ECs, including CD26 and placenta growth factor (Fig. 3A). Interestingly, we found that heparin-binding EGF-like growth factor (HB-EGF), a well known proangiogenic growth factor (17, 18), was specifically up-regulated (approximately threefold) in PAR-2–stimulated hypoxic HUVECs, whereas hypoxia alone or PAR-2 stimulation at normoxic conditions had virtually no effect on HB-EGF levels (Fig. 3A). These results were supported by increased immunofluorescence staining for HB-EGF and substantially increased HB-EGF mRNA expression by PAR-2AP stimulation at hypoxia, both in HUVECs and in HBMECs (Fig. 3B and Fig. S4). PAR-2–dependent induction of HB-EGF protein as well as mRNA was efficiently counteracted by p-ERK1/2 inhibition (Fig. 3 C and D). Heparin, which is known to inhibit HB-EGF activity through interference with heparan sulfate proteoglycan binding (19), reversed PAR-2–dependent proliferation of ECs (Fig. 3E). Heparin could potentially interfere with the activity of several other angiogenic growth factors in ECs; however, at the conditions used, heparin specifically inhibited PAR-2–activated ECs (Fig. 3E). Moreover, antibody-mediated blockage of HB-EGF significantly counteracted PAR-2–dependent proliferation and scratch wound closure of ECs (Fig. 3 F and G). These results indicate that HB-EGF has a functional role in hypoxia-driven, PAR-2/ERK1/2–dependent activation of ECs.

Cancer Cell-Derived Vesicles Trigger ECs in a TF-Dependent Manner.
The TF/VIIa protease complex is known to induce PAR-2 signaling through proteolytic cleavage of its extracellular N terminus (20); however, TF is considered virtually absent in normal endothelium (21). Indeed, we found that TF was undetectable in HUVECs as well as in HUAECs at normoxic conditions. Intriguingly, this was true also at hypoxic conditions (Fig. S5). These results indicated that neither normoxic nor hypoxic ECs can trigger TF-dependent PAR-2 signaling in a cell-autonomous manner.

Previous reports have shown that various types of cells, including malignant cells, secrete TF associated with microvesicles (MVs) that, depending on their size, origin, and composition, are denoted as microparticles, ectosomes, or exosomes (22–24). We hypothesized that GBM cells may activate hypoxic ECs in a paracrine manner through the secretion of TF-bearing MVs. In contrast to ECs, TF protein and mRNA were substantially induced by hypoxia in human GBM cells (U87-MG; Fig. S6 A and B). Confocal microscopy analysis suggested that TF in hypoxic GBM cells was mainly located at or near the plasma membrane (Fig. S6C), as supported by a concordant increase of TF procoagulative activity (Fig. S6D). We similarly found substantial, hypoxic induction of TF mRNA and protein in human lung cancer cells (Fig. S6 E and F). Hypoxic induction of TF was associated with dramatically increased TF levels in the medium of GBM cells (Fig. S7A). The vast majority (approximately 80%) of TF in GBM cell culture medium was associated with the vesicular fraction (Fig. S7B). EM of vesicle-enriched fractions showed intact MVs that were typically 60 to 100 nm in size. In addition to TF, isolated MVs stained positive for the tetraspanins CD63 and CD81 (Fig. S7C), which are well known markers of exosomes (25). These results were corroborated by immunoblotting experiments, which showed the enrichment of TF, CD81, and CD63 and depletion of the ER marker calnexin in MVs compared with whole cell lysates (Fig. S7D). Interestingly,
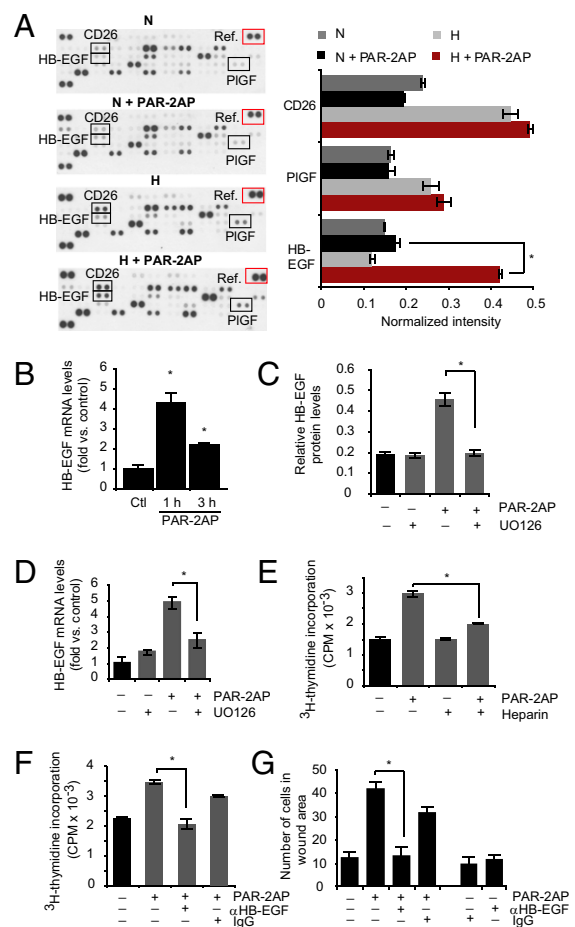

Fig. 3. PAR-2–mediated stimulation of hypoxic ECs involves p-ERK1/2–dependent induction of HB-EGF. (A) PAR-2–mediated induction of HB-EGF in hypoxic ECs. Normoxic (N) or hypoxic (H) HUVECs were incubated with or without PAR2-AP (100 μM) for 6 h, and angiogenesis-related proteins were determined by antibody array analysis as described in *SI Materials and Methods*. *Left*: Representative immunoblot from three independent experiments. *Right*: Quantification of placenta growth factor (PlGF), CD26, and HB-EGF levels at the various conditions presented as relative intensities versus array reference (red box). (*P < 0.05.) (B) Hypoxic HUVECs were incubated without (Ctl) or with PAR2-AP (100 μM) for 1 h or 3 h; HB-EGF mRNA expression was determined by qRT-PCR. (*Significant up-regulation vs. control, *P < 0.05.) (C) PAR-2–mediated HB-EGF induction depends on p-ERK1/2. Hypoxic HUVECs were untreated or pretreated with UO126, followed by another incubation period with or without PAR-2AP (100 μM) for 6 h. HB-EGF protein levels were quantified by immunoblotting as in A. (*P < 0.05.) (D) Similar experiment as in C showing HB-EGF mRNA expression as determined by qRT-PCR. (*P < 0.05.) Under the conditions used, UO126 efficiently inhibited PAR-2AP–induced p-ERK1/2 (Fig. S3B). (E–G) Role of HB-EGF in PAR-2–mediated activation of hypoxic ECs. (E) Hypoxic HUVECs were cultured for 24 h, starved for 16 h, and then untreated or treated with PAR-2AP (100 μM) and/or heparin (1 ng/mL) as indicated for another 24 h in the presence of 3 μCi/mL [³H]thymidine. (*P < 0.05.) (F) Similar experiment as in E; hypoxic HUVECs were untreated or treated with PAR-2AP and/or anti–HB-EGF antibody (12.5 μg/mL) as indicated. Nonimmune IgG (12.5 μg/mL) was used as a negative control. (*P < 0.05.) (G) Hypoxic HUVECs were cultured for 24 h and starved for 16 h, and then a scratch wound was formed in confluent monolayers, followed by another 36 h of migration with the treatments indicated. The results are presented as the mean number of cells per wound area ± SD. (*P < 0.05.)

we were able to demonstrate significant levels of VIIa in exosome-like MVs from hypoxic GBM cells (Fig. S7E), and MVs were able to generate active Xa even in the absence of exogenous VIIa (Fig. S7F). MVs were, however, negative for PAR-2 (Fig. S7E).
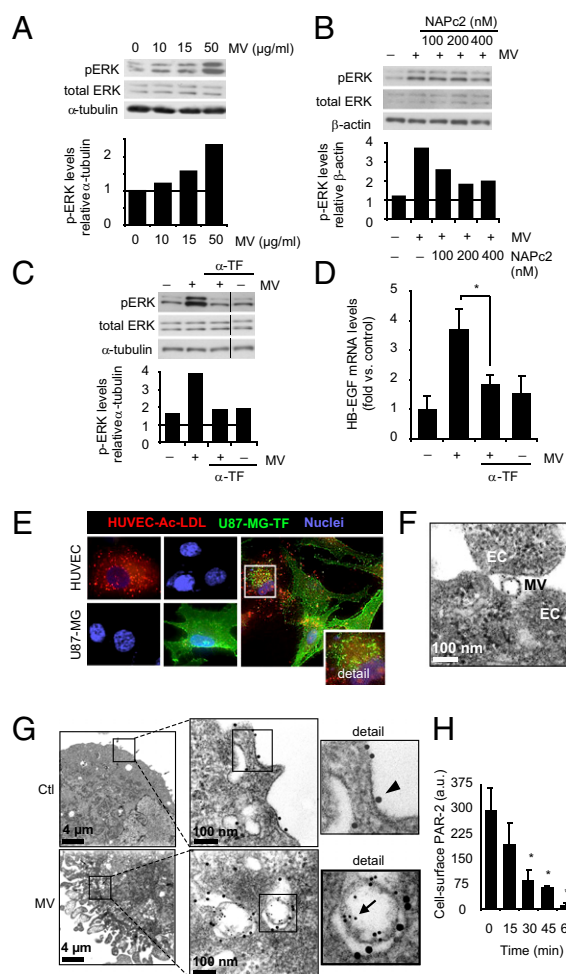
CELL BIOLOGY

Fig. 4. TF-bearing MVs trigger p-ERK1/2 and HB-EGF and colocalize with PAR-2 in hypoxic ECs. (*A–D*) MVs from hypoxic GBM cells trigger p-ERK1/2 and HB-EGF in hypoxic ECs in a TF-dependent manner. (*A*) MVs isolated from hypoxic U87-MG cells were incubated with HUVECs at the indicated concentrations for 5 min, followed by immunoblotting for p-ERK1/2, total ERK1/2, and α-tubulin. *Lower*: p-ERK/α-tubulin ratios from a representative experiment. (*B*) Hypoxic HUVECs were untreated or incubated with MVs (10 μg/mL) from hypoxic U87-MG cells for 5 min in the absence or presence of increasing concentrations of NAPc2 as indicated. Shown are immunoblots for p-ERK1/2, total ERK1/2, and β-actin. *Lower*: p-ERK/β-actin ratios from a representative experiment. (*C*) Hypoxic HUVECs were untreated or treated with MV as in *B* in the absence or presence of anti-human TF antibody (α-TF; 1:100), followed by immunoblotting for p-ERK1/2, total ERK1/2, and α-tubulin. *Lower*: p-ERK/α-tubulin ratios from a representative experiment. (*D*) Hypoxic HUVECs were incubated without or with MVs (10 μg/mL) for 1 h in the absence or presence of α-TF (1:100); HB-EGF mRNA expression was determined by qRT-PCR. (*P < 0.05.) (*E–H*) Vesicular transfer of TF from GBM cells into a PAR-2–containing compartment of ECs. (*E*) Confocal microscopy of U87-MG cells and HUVECs cultured in hypoxia for 24 h in the presence of the EC marker Ac-LDL (red). Cells were fixed and stained for TF (green) and nuclei (blue). HUVECs were positive for Ac-LDL and negative for TF, whereas the reverse was found in U87-MG cells. *Right*: Coincubation experiment with U87-MG cells and HUVECs in hypoxia for 24 h. Detail shows representative HUVEC containing TF-positive vesicular structures. (*F*) MVs (40 μg/mL) isolated from hypoxic U87-MG cells were incubated with hypoxic HUVECs for 30 min, and ECs were analyzed by Immunogold labeling for TF and EM as described in *Materials and Methods*. Shown is a TF-positive MV at the surface of ECs. (*G*) Hypoxic HUVECs were incubated without (Ctl) or with MVs from hypoxic U87-MG cells for 30 min, and then analyzed by Immunogold labeling for TF (5-nm gold particle, arrow) and PAR-2 (15-nm gold particle, arrowhead), followed by EM analysis. *Upper*: PAR-2 staining at the EC surface. *Lower*: Localization of TF-labeled MVs in a PAR-2–positive compartment of ECs. (*H*) MVs (10 μg/mL) time-dependently induce PAR-2 internalization in hypoxic HUVECs, as determined by EC surface staining for PAR-2 and flow cytometry. Data are presented as average ± SD. (*P < 0.05.)

These results indicated that MVs from hypoxic GBM cells carry TF and VIIa with the potential to activate PAR-2 signaling in ECs. In support of this notion, MVs were shown to induce p-ERK1/2 (Fig. 4*A*) and HB-EGF (Fig. 4*D* and Fig. S8) in ECs, and to stabilize EC tube structures and thus counteract tube disintegration at hypoxic conditions (Fig. S8*C*). Confocal microscopy analysis showed the transfer of TF to vesicular structures of ECs coincubated with GBM cells at hypoxic conditions (Fig. 4*E*); EM studies confirmed EC uptake of TF-loaded MVs (Fig. 4 *F* and *G*) that colocalized with PAR-2 in target ECs. Moreover, we found that cell-surface PAR-2 internalization in hypoxic ECs was efficiently induced by GBM cell-derived MVs (Fig. 4*H*). In further support of an involvement of TF in MV-mediated EC activation, the nematode anticoagulant protein c2 (NAPc2), a potent inhibitor of the TF/VIIa complex (26), was found to partially reverse MV-mediated induction of p-ERK1/2 (Fig. 4*B*) and EC proliferation (Fig. 5*A*). More importantly, antibody-mediated blockage of TF was found to reverse MV-dependent induction of p-ERK1/2 (Fig. 4*C*), HB-EGF (Fig. 4*D*), and EC proliferation (Fig. 5*B*). Finally, the addition of exogenous VIIa reinforced the induction of p-ERK1/2 as well as the stimulation of EC proliferation by MVs (Fig. 5 *C* and *D*).

Discussion

Cancer cell-derived MVs and their role in intercellular communication in the tumor microenvironment is an emerging concept in the cancer field (22–25, 27–30). A communication route based on MVs may provide malignant cells with a highly versatile system to influence the surrounding microenvironment during angiogenesis, invasion, and metastasis, as well as for immune surveillance. Here, we provide evidence that GBM cell-derived MVs may constitute an important signaling mechanism in hypoxia-driven modulation of nonmalignant tumor cells. Our findings indicate that hypoxic cancer cells release TF/VIIa-bearing MVs that trigger up-regulated PAR-2 on hypoxic vascular ECs, which results in increased levels of the proangiogenic growth factor HB-EGF (Fig. 5*E* shows a schematic summary).

Of particular interest in the context of the present investigation, it has been shown that GBM-derived MVs stimulate EC tube formation; however, the underlying molecular mechanism of this effect was not elucidated (27). Others have shown that MVs can transfer the oncogenic form of the EGFR, EGFRvIII, between GBM cells (28) as well as from GBM cells to ECs (29), resulting in EGFRvIII-driven phenotypic modulation of recipient cells. Moreover, Antonyak et al. (30) recently showed that MVs from U87-MG cells could induce transformed cell characteristics in fibroblasts through the transfer of cross-linked tissue transglutaminase-fibronectin.

Significant findings of the present study are hypoxic induction of PAR-2 in ECs and hypoxia-driven EC activation through PAR-2 signaling. There appears to be a specific role for PAR-2, as PAR-1 expression was unaffected by hypoxia in ECs. Further, we show that PAR-2 in this context acts through a pathway involving ERK1/2-dependent induction of proangiogenic HB-EGF. These findings, and the fact that antibody-mediated neutralization of HB-EGF also has shown inhibitory effects in GBM cells (31), should motivate further in vivo studies exploring HB-EGF as a target in GBM therapy.

It was recently shown that glioma cells display increased cell migration and invasion under hypoxic conditions, which was associated with enhanced TF/VIIa-mediated PAR-2 activation (32), and that EGFRvIII transformed GBM cells become hypersensitive to TF/PAR-mediated signaling (10), indicating a role of this pathway also in autocrine stimulation of GBM cells. Whereas malignant transformation appears to induce TF as well as PARs (10), we found that hypoxia specifically up-regulates TF, and rather down-regulates PAR-2 expression in GBM cells (Fig. S9). There thus appears to be a complex interaction be-
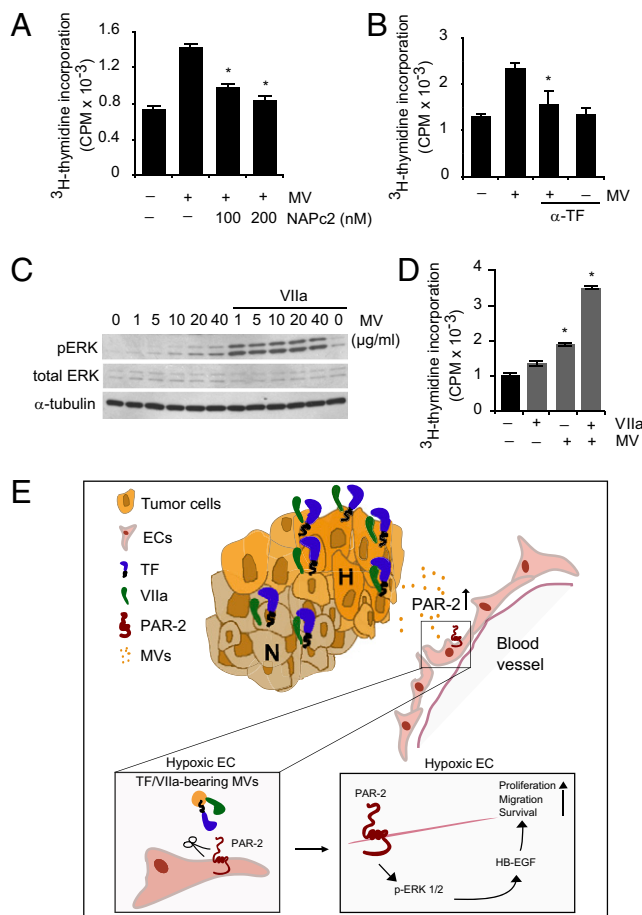
Fig. 5. MV-mediated activation of hypoxic ECs is TF/VIIa-dependent. (*A* and *B*) Hypoxic HUVECs were untreated or incubated with MVs (0.1 μg/mL) in the absence or presence of NAPc2 (*A*) or anti-human TF antibody (α-TF, *B*) as indicated for 72 h in the presence of 3 μCi/mL [³H]thymidine. Cell proliferation was determined by [³H]thymidine incorporation. (*Significantly different from MV stimulation in the absence of TF inhibitor, $P < 0.05$.) (*C*) MVs at the indicated concentrations with or without exogenous VIIa (4 nM) were incubated with hypoxic HUVECs for 5 min, followed by immunoblotting for p-ERK1/2, total ERK1/2, and β-actin. (*D*) Hypoxic HUVECs were treated with MVs with or without exogenous VIIa (4 nM) as indicated for 72 h, and cell proliferation was determined by [³H]thymidine incorporation. (*Significantly different from untreated control, $P < 0.05$.) (*E*) Hypoxic (H) GBM cells release MVs that are loaded with the TF/VIIa coagulation initiation protease complex; hypoxic ECs appear to be devoid of TF, which precludes cell-autonomous PAR-2 activation. PAR-2 is up-regulated by hypoxia in ECs that are activated by GBM cell-derived MVs in a paracrine manner through a pathway involving PAR-2/ERK1/2–dependent induction of the proangiogenic growth factor HB-EGF. We propose that MVs provide GBM cells with a powerful signaling mechanism in hypoxia-driven modulation of ECs, resulting in increased angiogenesis and accelerated tumor growth.

tween oncogenetic events and nononcogenetic events, i.e., hypoxia, in coagulation-dependent PAR signaling in GBM cells.

Several stimuli, e.g., shear stress, cytokines, and growth factors, have been shown to transiently induce TF in ECs. The fact that TF was undetectable in hypoxic ECs is thus intriguing; future studies should explore the possibility that functional TF, in analogy with EGFRvIII (28, 29), may be incorporated from cancer cell-derived MVs into ECs to trigger PAR-2 in a cell-autonomous manner. This may occur locally in the tumor, but potentially also at the systemic level, as tumor-derived vesicles have been shown to escape into the bloodstream of patients with cancer (33). Notably, in a human GBM xenograft SCID mouse

model, we found that plasma levels of human TF correlated with tumor mass, suggesting that TF secreted by GBM cells escapes into the circulation (Fig. S10). An interesting, yet hypothetical, possibility is that TF-enriched MVs secreted from hypoxic GBM cells are the underlying mechanism of the high incidence of thromboembolism in GBM; perhaps more importantly, circulating, MV-associated TF may provide a noninvasive marker that reflects a more hypoxic and aggressive tumor.

In summary, this study provides insight into how the phenotypic characteristics of GBM may interact at the molecular level during tumor development. We show that hypoxia orchestrates a paracrine pathway that involves cancer cell-derived, procoagulative MVs and the induction of PAR-2/ERK1/2/HB-EGF–dependent activation of ECs.

Materials and Methods

Materials and descriptions of angiogenesis and phosphokinase arrays, immunoblotting, immunofluorescence microscopy, lactate dehydrogenase (LDH) release, Matrigel tube formation, quantitative real-time PCR (qRT-PCR), RNAi experiments, and TF ELISA and TF activity assays are listed in *SI Materials and Methods*.

Cell Culture. HUVEC and HUAEC cells (purchased from Lonza) were cultured in EC basal medium supplemented with 10% heat-inactivated FBS, 2 mM L-glutamine, 100 U/mL penicillin, 100 μg/mL streptomycin, 10 ng/mL hydrocortisone, and 20 μg/mL human recombinant EGF (growth medium). HBMEC cells (purchased from 3H Biomedical) were cultured in EC medium supplemented with 5% FBS, 100 U/mL penicillin, 100 μg/mL streptomycin, and EC growth supplement. Human GBM (U87-MG) cells and human lung carcinoma (A549) cells (purchased from ATCC) were cultured in DMEM and F12K, respectively, supplemented with 10% FBS, 2 mM L-glutamine, 100 U/mL penicillin, and 100 μg/mL streptomycin. All cells were cultured in a humidified incubator set at 5% CO_2 and 37 °C. For hypoxia experiments, cells were incubated in a humidified InVivo₂ Hypoxia Workstation 400 (Ruskinn Technology) set at 5% CO_2, 94% N_2, 1% O_2, and 37 °C.

Proliferation and Migration Assays. HUVECs were incubated in normoxia or hypoxia for 24 h in growth medium and starved in serum-free medium for 16 h, followed by the various treatments as described later with continuous incubation at normoxia or hypoxia. For proliferation, starved HUVECs were untreated or treated with 100 μM PAR-1AP, 100 μM PAR-2AP, and/or 12.5 μg/mL anti–HB-EGF blocking antibody for 24 h, or with 0.1 μg/mL MVs with or without 4 nM VIIa for 48 h, in EBM supplemented with 1% heat-inactivated FBS and 3 μCi/mL [³H]thymidine. The amount of incorporated [³H]thymidine was determined by Beckman Coulter LS6500 liquid scintillation as previously described (34). For scratch assay, a wound was formed in starved HUVEC monolayers with a sterile plastic pipette followed by extensive washing. Cells were then left untreated or treated with 100 μM PAR-1AP or 100 μM PAR-2AP in EBM with 1% heat-inactivated FBS for 36 h. Wound closure was measured by counting the number of cells in the wound area in nine separate replicates in each group. Cells were captured using a Leitz Fluovert FS microscope equipped with a 10× objective and a digital camera. For transwell assay, starved, hypoxic HUVECs were seeded in serum-free medium into 8-μm pore cell culture inserts precoated with 10 μg/mL fibronectin. Cells were left untreated or treated with 100 μM PAR-2AP with or without 12.5 μg/mL HB-EGF blocking antibody. Cells were allowed to migrate for 5 h and were subsequently stained with crystal violet and quantified as previously described (35). In all experiments with blocking antibody, equal protein amounts of mouse, nonimmune IgG were used as control.

MV Purification and Characterization. Secreted vesicles were isolated from cell culture medium as previously described (27, 29, 30, 36). Briefly, U87-MG cells were cultured at normoxic or hypoxic conditions for the time periods as indicated in figure legends in serum-free medium supplemented with 1% BSA (wt/vol). Collected cell culture medium from subconfluent 175-cm² flasks was depleted of cells and cell debris by consecutive, low-speed centrifugations. The obtained supernatants were carefully collected and centrifuged for 2 h at 100,000 × *g* at 4 °C. Pellets from this centrifugation step were washed in PBS solution and centrifuged for 70 min at 100,000 × *g* at 4 °C, and the obtained pellets were resuspended in PBS solution. The nature of isolated MVs was studied by transmission electron microscopy (as detailed later) and immunoblot analysis (*SI Materials and Methods*), showing no organelle contamination as determined by the absence of ER/Golgi

markers, and the strong enrichment of the exosomal markers CD63 and CD81 (25).

Confocal Laser Scanning Microscopy. For antibody stainings, subconfluent HUVECs in eight-well chamber slides were fixed with 2% paraformaldehyde for 10 min, washed with PBS solution/BSA 1% (wt/vol) and blocked with PBS solution/BSA for 30 min followed by staining with mouse monoclonal anti-PAR-2 (1:200; no. 13504; Santa Cruz), anti–PAR-1 (1:200; no. 13503; Santa Cruz), or anti-TF (1:200; 10H10) antibody at 4 °C overnight, and subsequently stained with goat anti-mouse Alexa Fluor 488 (1:200; Invitrogen) for 30 min at room temperature. Cells were counterstained for F-actin by using phalloidin-TRITC and/or Hoechst 33342 nuclear stain, followed by mounting in Aqua Pertex (Histolab). In some experiments, HUVECs were pretreated with 10 μg/mL MVs for 6 h, washed extensively with 1 M NaCl to remove nonspecifically bound MVs, fixed, and stained with rabbit polyclonal HB-EGF antibody (1:200; no. 16783; Abcam) at 4 °C overnight, and subsequently stained with goat anti-rabbit Alexa Fluor 488 (1:200; Invitrogen) for 30 min at room temperature. In coculture experiments, HUVECs and U87-MG cells were seeded simultaneously (HUVEC,U87-MG ratio 1:5) in serum-free medium and cultured at hypoxia for 24 h. Acetylated-LDL-rhodamine (Ac-LDL; 4 μg/mL) was added for 3 h before fixation and staining for TF and nuclei as described earlier. Cells were analyzed by using a Zeiss LSM 710 confocal scanning microscope equipped with a 20× objective. Controls without respective primary antibody were included in all experiments.

EM. Isolated MVs and cells were washed twice in Tris-buffered saline solution, pelleted, and fixed for 1 h at 20 °C and overnight at 4 °C in 2.5% glutaraldehyde in cacodylate buffer. Cells were washed with cacodylate buffer, postfixed for 1 h at 20 °C in 1% osmium tetroxide in cacodylate buffer, dehydrated in a graded series of ethanol, and then embedded in Epon 812 with acetone as an intermediate solvent. Specimens were analyzed for negative staining or cut into 50-nm sections on an LKB ultramicrotome, and stained with uranyl acetate and lead citrate. Some samples were incubated with anti-TF (1:50) and/or anti–PAR-2 (1:100) antibodies, followed by secondary antibodies conjugated with 5 nm gold (1:10) or 15 nm gold (1:20) from Electron Microscopy Sciences. Specimens were examined in a JEM 1230 transmission electron microscope (JEOL) at 80 kV accelerating voltage. Images were captured with a Gatan Multiscan 791 CCD camera.

Statistical Analyses. Data are presented as the mean ± SD ($n = 3–6$). Statistical significance was evaluated with the Student t test using Microsoft Excel; a P value lower than 0.05 was considered significant.

1. Stupp R, et al.; European Organisation for Research and Treatment of Cancer Brain Tumour and Radiation Oncology Groups; National Cancer Institute of Canada Clinical Trials Group (2009) Effects of radiotherapy with concomitant and adjuvant temozolomide versus radiotherapy alone on survival in glioblastoma in a randomised phase III study: 5-year analysis of the EORTC-NCIC trial. *Lancet Oncol* 10:459–466.
2. Evans SM, et al. (2004) Hypoxia is important in the biology and aggression of human glial brain tumors. *Clin Cancer Res* 10:8177–8184.
3. Brown JM, Wilson WR (2004) Exploiting tumour hypoxia in cancer treatment. *Nat Rev Cancer* 4:437–447.
4. Brat DJ, Van Meir EG (2004) Vaso-occlusive and prothrombotic mechanisms associated with tumor hypoxia, necrosis, and accelerated growth in glioblastoma. *Lab Invest* 84:397–405.
5. Belting M, Ahamed J, Ruf W (2005) Signaling of the tissue factor coagulation pathway in angiogenesis and cancer. *Arterioscler Thromb Vasc Biol* 25:1545–1550.
6. Rak J, Yu JL, Luyendyk J, Mackman N (2006) Oncogenes, trousseau syndrome, and cancer-related changes in the coagulome of mice and humans. *Cancer Res* 66:10643–10646.
7. Hamada K, et al. (1996) Expression of tissue factor correlates with grade of malignancy in human glioma. *Cancer* 77:1877–1883.
8. Milsom CC, et al. (2008) Tissue factor regulation by epidermal growth factor receptor and epithelial-to-mesenchymal transitions: Effect on tumor initiation and angiogenesis. *Cancer Res* 68:10068–10076.
9. Rong Y, et al. (2009) Epidermal growth factor receptor and PTEN modulate tissue factor expression in glioblastoma through JunD/activator protein-1 transcriptional activity. *Cancer Res* 69:2540–2549.
10. Magnus N, Garnier D, Rak J (2010) Oncogenic epidermal growth factor receptor upregulates multiple elements of the tissue factor signaling pathway in human glioma cells. *Blood* 116:815–818.
11. Rong Y, et al. (2006) Early growth response gene-1 regulates hypoxia-induced expression of tissue factor in glioblastoma multiforme through hypoxia-inducible factor-1-independent mechanisms. *Cancer Res* 66:7067–7074.
12. Camerer E, Huang W, Coughlin SR (2000) Tissue factor- and factor X-dependent activation of protease-activated receptor 2 by factor VIIa. *Proc Natl Acad Sci USA* 97:5255–5260.
13. Belting M, et al. (2004) Regulation of angiogenesis by tissue factor cytoplasmic domain signaling. *Nat Med* 10:502–509.
14. Uusitalo-Jarvinen H, et al. (2007) Role of protease activated receptor 1 and 2 signaling in hypoxia-induced angiogenesis. *Arterioscler Thromb Vasc Biol* 27:1456–1462.
15. Bohm SK, et al. (1996) Molecular cloning, expression and potential functions of the human proteinase-activated receptor-2. *Biochem J* 314:1009–1016.
16. Frungieri MB, Weidinger S, Meineke V, Köhn FM, Mayerhofer A (2002) Proliferative action of mast-cell tryptase is mediated by PAR2, COX2, prostaglandins, and PPAR-gamma: Possible relevance to human fibrotic disorders. *Proc Natl Acad Sci USA* 99:15072–15077.
17. Higashiyama S, Abraham JA, Miller J, Fiddes JC, Klagsbrun M (1991) A heparin-binding growth factor secreted by macrophage-like cells that is related to EGF. *Science* 251:936–939.
18. Ongusaha PP, et al. (2004) HB-EGF is a potent inducer of tumor growth and angiogenesis. *Cancer Res* 64:5283–5290.
19. Higashiyama S, Abraham JA, Klagsbrun M (1993) Heparin-binding EGF-like growth factor stimulation of smooth muscle cell migration: dependence on interactions with cell surface heparan sulfate. *J Cell Biol* 122:933–940.
20. Coughlin SR (2000) Thrombin signalling and protease-activated receptors. *Nature* 407:258–264.
21. Kasthuri RS, Taubman MB, Mackman N (2009) Role of tissue factor in cancer. *J Clin Oncol* 27:4834–4838.
22. Belting M, Wittrup A (2008) Nanotubes, exosomes, and nucleic acid-binding peptides provide novel mechanisms of intercellular communication in eukaryotic cells: implications in health and disease. *J Cell Biol* 183:1187–1191.
23. Al-Nedawi K, Meehan B, Rak J (2009) Microvesicles: Messengers and mediators of tumor progression. *Cell Cycle* 8:2014–2018.
24. Cocucci E, Racchetti G, Meldolesi J (2009) Shedding microvesicles: Artefacts no more. *Trends Cell Biol* 19:43–51.
25. Mathivanan S, Ji H, Simpson RJ (2010) Exosomes: Extracellular organelles important in intercellular communication. *J Proteomics* 73:1907–1920.
26. Lee AY, Vlasuk GP (2003) Recombinant nematode anticoagulant protein c2 and other inhibitors Targeting blood coagulation factor VIIa/tissue factor. *J Intern Med* 254:313–321.
27. Skog J, et al. (2008) Glioblastoma microvesicles transport RNA and proteins that promote tumour growth and provide diagnostic biomarkers. *Nat Cell Biol* 10:1470–1476.
28. Al-Nedawi K, et al. (2008) Intercellular transfer of the oncogenic receptor EGFRvIII by microvesicles derived from tumour cells. *Nat Cell Biol* 10:619–624.
29. Al-Nedawi K, Meehan B, Kerbel RS, Allison AC, Rak J (2009) Endothelial expression of autocrine VEGF upon the uptake of tumor-derived microvesicles containing oncogenic EGFR. *Proc Natl Acad Sci USA* 106:3794–3799.
30. Antonyak MA, et al. (2011) Cancer cell-derived microvesicles induce transformation by transferring tissue transglutaminase and fibronectin to recipient cells. *Proc Natl Acad Sci USA* 108:4852–4857.
31. Ramnarain DB, et al. (2006) Differential gene expression analysis reveals generation of an autocrine loop by a mutant epidermal growth factor receptor in glioma cells. *Cancer Res* 66:867–874.
32. Gessler F, et al. (2010) Inhibition of tissue factor/protease-activated receptor-2 signaling limits proliferation, migration and invasion of malignant glioma cells. *Neuroscience* 165:1312–1322.
33. Graner MW, et al. (2009) Proteomic and immunologic analyses of brain tumor exosomes. *FASEB J* 23:1541–1557.
34. Welch JE, et al. (2008) Single chain fragment anti-heparan sulfate antibody targets the polyamine transport system and attenuates polyamine-dependent cell proliferation. *Int J Oncol* 32:749–756.
35. Kucharzewska P, Welch JE, Svensson KJ, Belting M (2010) Ornithine decarboxylase and extracellular polyamines regulate microvascular sprouting and actin cytoskeleton dynamics in endothelial cells. *Exp Cell Res* 316:2683–2691.
36. Pegtel DM, et al. (2010) Functional delivery of viral miRNAs via exosomes. *Proc Natl Acad Sci USA* 107:6328–6333.